This is the author's peer reviewed, accepted manuscript. However, the online version of record will be different from this version once it has been copyedited and typeset

PLEASE CITE THIS ARTICLE AS DOI: 10.1063/5.0173978

Infrared Dielectric Function of $GaAs_{1-x}P_x$ Semiconductor Alloys Near the Reststrahlen Bands

Stefan Zollner, ^{1, a)} Shivashankar R. Vangala, ² Vladimir L. Tassev, ² Duane Brinegar, ^{2, 3} and Samuel Linser^{2, 3} ¹⁾ Department of Physics, New Mexico State University, MSC 3D, PO Box 30001, Las Cruces, NM 88003-8001, USA

²⁾ Air Force Research Laboratory (AFRL), Sensors Directorate, Wright-Patterson AFB, OH 45433,

USA

3) KBR, Inc., Beavercreek, OH, 45431, USA

(Dated: 6 October 2023)

The infrared dielectric function of thick $GaAs_{1-x}P_x$ alloy layers grown on (001) GaAs substrates by hydride vapor phase epitaxy was investigated in the reststrahlen region using Fourier-transform infrared ellipsometry. The spectra are influenced by the Berreman artifact at the longitudinal optical phonon frequency of the GaAs substrate and by interference fringes due to the finite layer thickness. The ellipsometric angles were analyzed to determine the dielectric function of the alloy layer. Two-mode behavior including strong GaAs-like and GaP-like optical phonons was observed, confirming the results of Verleur and Barker (Phys. Rev. 149, 715, 1966). Due to the increased sensitivity of ellipsometry in the reststrahlen region, several weak phonon features could also be seen. The lattice absorption peaks are asymmetric and show side bands at the lower and higher frequencies. A single additional peak, as suggested by the percolation model, does not describe the spectra. The cluster model proposed by Verleur and Barker is a better fit to the data. Due to the broadening of the phonon absorption peaks, the authors were unable to find a unique decomposition into multiple components.

The long-wavelength optical phonons of compound semiconductor alloys have long been an active area of research. While the infrared (IR) lattice response of binary zincblende compounds like GaAs¹⁻⁴ and GaP⁴⁻⁶ can be described quite well with a simple Lorentzian resulting in one reststrahlen band between the transverse optical (TO) and longitudinal optical (LO) phonon energies, at least two such reststrahlen bands are found in many semiconductor alloys. Genzel, Martin, and Perry⁷ explained that the long-wavelength phonons of mixed crystals can be represented by four classes, which they called one-mode, two-mode, and intermediate. The early experimental evidence was reviewed by Chang and Mitra.⁸

GaAs_{1-x}P_x alloys display two-mode behavior:^{7,8} Since the reststrahlen bands of GaAs and GaP are separated by a large energy gap (73 cm⁻¹), two distinct GaAs-like and GaP-like phonon bands appear in the alloy over the complete range of compositions. These bands shift with composition, but they never overlap. As pointed out by Humlíček,⁹ IR reflection (including ellipsometry) measurements are very sensitive to weak absorption processes within the reststrahlen band. Therefore, several smaller IR absorption peaks were also detected in $GaAs_{1-x}P_x$ alloys,^{10,11} but could not be explained with two-phonon absorption. Weak secondary peaks were also found in Raman scattering experiments. ^{12,13} Different explanations were given for these weak peaks, especially the cluster model^{10,14} and the percolation model. ¹⁵

While theoretical interest in the nature of these weak peaks has continued, 14,15 calculations are still compared to 50 year-old IR reflectance data. 10 Therefore, a reexamination of the IR lattice response of ${\rm GaAs}_{1-x}{\rm P}_x$ al-

loys using modern IR ellipsometry equipment is overdue. That is the purpose of this manuscript. Our measurements of thick relaxed epitaxial layers grown on GaAs lead to a minor inconvenience, the Berreman artifact at the LO mode of the substrate and interference fringes due to the finite thickness, but this can be resolved with optical modeling of the thin-film response. As far as we know, alloy phonons have only been studied previously with IR ellipsometry for wurtzite semiconductor nitride alloys 16,17 and for various metal oxides with low crystal symmetry, 18 but not for zincblende semiconductor alloys.

 $GaAs_{1-x}P_x$ alloys have been used historically for red light emitting diodes. 19 More recent interest has been for compact, high-power, tunable laser sources for middle to long wavelength IR (3-14 μ m) operation, which are in great demand for a wide variety of applications.^{20,21} These include critical military applications such as proactive and post launch IR countermeasures, enhanced laser radar for ranging, target recognition, and 3D holography, and reliable long-range IR communication, as well as applications in security such as remote sensing and spectroscopy of chemicals and biological species, medical applications like breath analysis, and science applications like ultrafast spectroscopy of chemical reaction dynamics. However, since the available direct coherent sources in this spectral range do not satisfy requirements for power, tunability, and frequency coverage associated with such applications, frequency conversion through phase or quasi-phase matching in nonlinear optical materials was suggested as a reasonable alternative for developing such sources for this important frequency range. $GaAs_{1-x}P_x$ as a combination of two of the most studied to date quasi-phase matching materials, GaAs and GaP, is especially attractive by the possibility to engineer a material with lower two-photon absorption than GaAs but

 $^{^{\}rm a)}{\rm zollner@nmsu.edu};$ http://femto.nmsu.edu

This is the author's peer reviewed, accepted manuscript. However, the online version of record will be different from this version once it has been copyedited and typeset

PLEASE CITE THIS ARTICLE AS DOI: 10.1063/5.0173978

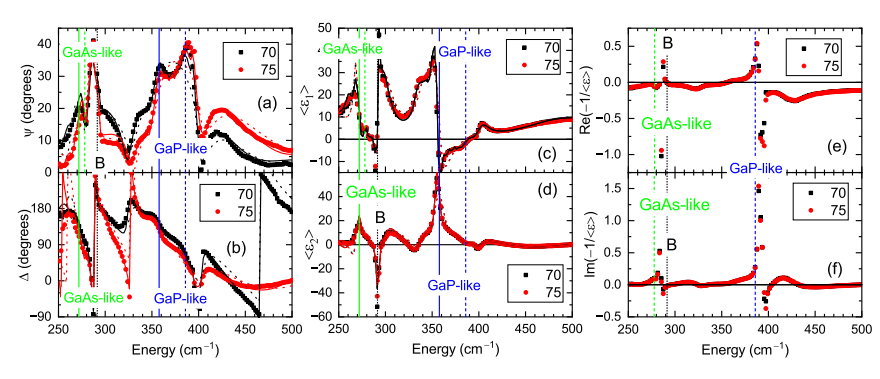


FIG. 1. Ellipsometric angles ψ (a) and Δ (b), real (c) and imaginary (d) parts of the pseudodielectric function and of the pseudoloss function (e,f) for sample 225B with 61.5% P. The symbols show experimental data at two angles of incidence. The dotted vertical line labelled "B" indicates the Berreman artifact at the LO energy of the GaAs substrate. The green and blue lines show the energies of the TO (solid) and LO (dashed) phonons of the GaAs-like and GaP-like phonons of the alloy. Fits to the data with two and eight Lorentzians are given by dotted and solid lines, respectively.

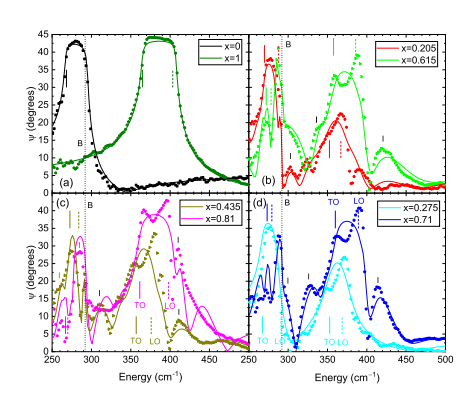


FIG. 2. The reststrahlen bands expressed by the ellipsometric angle ψ (symbols) measured at an incidence angle of 70° for bulk GaAs and GaP (a) and for thick $GaAs_{1-x}P_x$ alloys on GaAs (b,c,d). Solid lines show the best fit with a single Lorentzian for the GaAs-like and GaP-like optical phonons. The vertical dotted line shows the energy of the LO phonon in the GaAs substrate at $292~{\rm cm}^{-1}$, which causes a Berreman artifact for some samples. The short solid and dashed vertical lines mark the energies of the TO and LO modes, respectively. Peaks labelled "I" are interference fringes

higher nonlinear susceptibility than GaP, a material that could be, eventually, pumped with the readily available sources from the telecommunication waveband. The use of $GaAs_{1-x}P_x$ alloys for multijunction solar cells has also been discussed.²²

Thick $GaAs_{1-x}P_x$ alloy layers with compositions ranging from x=0.20 to 0.80 were grown by low-pressure hydride vapor phase epitaxy (HVPE) on (001) oriented GaAs substrates as described elsewhere. $^{21-24}$ This growth method is very fast and some variations in composition should be expected. This becomes apparent in x-ray diffraction (XRD) and ellipsometry measurements near the direct band gap. The alloy composition was determined using high-resolution XRD and roomtemperature photoluminescence.²⁵ A linear variation of the lattice constant with composition (Vegard's Law) was assumed. 10 We described the variation of the direct band gap of $GaAs_{1-x}P_x$ alloys with the bowing parameter of b=-0.19 eV recommended in Ref. 26, within the range of parameters determined by electroreflectance.^{27,28} A list of samples is given in Table SI. A few samples only produced diffuse reflections from a red alignment laser, but nevertheless had good IR ellisometry spectra.

The ellipsometric angles²⁹ ψ and Δ of several thick $GaAs_{1-x}P_x$ alloy layers on GaAs were acquired at room temperature from 250 to $8000~\mathrm{cm^{-1}}$ using a J. A. Woollam Fourier-transform IR variable angle of incidence spectroscopic ellipsometer (FTIR-VASE) as described in the Supplementary Material. Since ellipsometry measures two parameters (an amplitude $\tan \psi$ and a phase Δ) at each wavelength and angle of incidence, it is usually possible to extract the real and imaginary parts of the dielectric function of the layer without a Kramers-Kronig transformation, if the complex dielectric function of the substrate and the layer thickness are known. One can also build models for the complex dielectric functions of the substrate and layer that depend on parameters as described below. A good introduction to spectroscopic ellipsometry is given in the textbook by Fujiawara and Collins.²⁹

The phonon parameters for the GaAs and GaP binary endpoints were determined with measurements on reference substrates as described in Ref. 6 by fitting with a

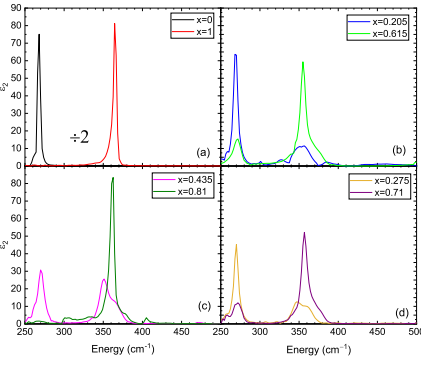


FIG. 3. Imaginary part of the dielectric function ϵ_2 for bulk GaAs and GaP (a) and for thick $GaAs_{1-x}P_x$ alloys on GaAs(b,c,d) determined from a B-spline fit to the ellipsometric angles. The spectra were divided by two for the bulk substrates in (a) to fit on the same scale as the alloys. The corresponding figure for the real part is shown in the Supplementary Material. Compare with Fig. 2 in Ref. 14.

simple Lorentzian

$$\epsilon \left(\omega \right) = \epsilon_{\infty} + \frac{A\Omega_{\rm TO}^2}{\Omega_{\rm TO}^2 - \omega^2 - i\Gamma_{\rm TO}\omega}.$$
 (1)

We did not find it necessary to include different broadening parameters for the transverse (TO) and longitudinal optical (LO) phonons due to anharmonic decay. The Lorentzian then has three parameters, the amplitude A, the TO phonon energy Ω_{TO} , and the broadening parameter Γ_{TO} . The energy of the corresponding LO phonon can be estimated from the Lyddane-Sachs-Teller relation⁶

$$\Omega_{\rm LO}^2 = \Omega_{\rm TO}^2 \left(\frac{A}{\epsilon_{\infty}} + 1 \right).$$
(2)

Equation (2) assumes frequency-independent screening of the Fröhlich interaction by the high-frequency dielectric constant ϵ_{∞} . This approximation is probably accurate for the GaP-like phonon with the higher energy. The GaAs-like phonon might be screened a little more, since the dielectric constant between the GaAs-like and GaP-like phonons is larger than ϵ_{∞} . Therefore, we might slightly overestimate the LO phonon energy of the GaAslike mode when using Eq. (2).

The ellipsometry data for a typical sample (225B) with a phosphorus content of 61.5%, within the percolation regime, 15 are shown in Fig. 1 in the reststrahlen region from 250 to 500 cm⁻¹ in several representations, as ellipsometric angles ψ and Δ , pseudodielectric function $\langle \epsilon \rangle$, and pseudoloss function $-1/\langle \epsilon \rangle$. A detailed interpretation of the raw data is given in the Supplementary Ma-

The spectrum was fitted with a sum of two Lorentzian oscillators to describe the GaAs-like and GaP-like

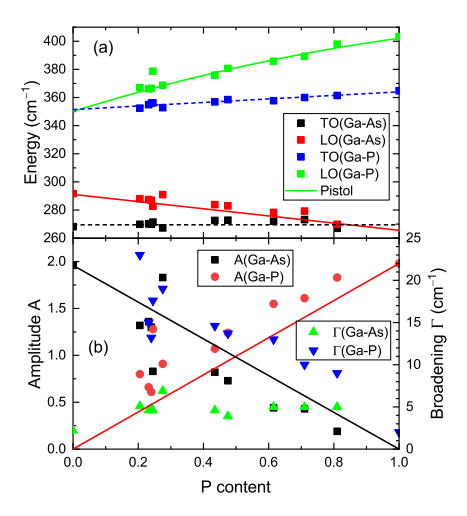


FIG. 4. (a) Energies of TO and LO phonons from FTIR ellipsometry (symbols) in comparison with the LO energies from Ref. 13 (solid) and a linear fit to the TO energies (dashed): (b) amplitudes and broadenings of TO phonons. Straight lines scale the amplitudes with composition.

phonons, shown by dotted lines in Fig. 1. Parameters obtained from the fit are given in Table SI. The corresponding LO energies were estimated from the Lyddane-Sachs-Teller relation (2). Solid vertical lines in Fig. 1 show the TO energies obtained from this fit. There is qualitative agreement, especially for the pseudodielectric function, but the agreement could be better. As expected, two Lorentzians are not sufficient to describe the complex vibrational spectra of the $GaAs_{1-x}P_x$ alloy.

The fit to the GaP-like band with a single Lorentzian (dotted) is particularly poor. As discussed by Humlíček,^{9,30} the impact of a weak absorption feature is amplified, if it occurs within a reststrahlen band. The shape of this GaP-like reststrahlen band allows the conclusion that the main GaP-like TO/LO phonon pair has energies of about 355 and 400 cm⁻¹, with a second weaker absorption peak located within these boundaries.

In summary, the main features of the raw ellipsometry data in Fig. 1 for sample 225B can be interpreted if the GaAs-like and GaP-like reststrahlen bands and the Berreman artifact^{31,32} at the TO energy of the GaAs substrate are taken into account. There are also small modifications due to the finite thickness of the alloy (interference effects).

Since a fit to the data with two Lorentzians to describe the GaAs-like and GaP-like vibrations was only partially successful, we added a second (weaker) GaPlike TO phonon, as suggested by the percolation theory of Pagès et al., 15 at an energy of about 12 cm⁻¹ above the stronger one. This reduced the mean standard dePLEASE CITE THIS ARTICLE AS DOI: 10.1063/5.0173978

viation (weighted by errors), also called MSE, by about 20%, but still did not provide a good description of ψ in the GaP-like reststrahlen region. The agreement between the model and the data for

sample 225B can be improved further if a total of eight Lorentzian oscillators are introduced to describe the lattice absorption. Results are shown by the solid lines in Fig. 1. Even such a large number of oscillators does not achieve a perfect fit to the data. It is questionable whether such a large number of Lorentzian parameters carries physical significance. We believe that our FTIR ellipsometry data do not contain enough information to perform meaningful fits with 6 to 10 Lorentzian for comparison with energies and amplitudes predicted by the cluster model theory, which was carried out in Ref. 14.

The ellipsometric angles ψ for six selected alloys and the binary endpoints are shown in Fig. 2 (symbols) together with the best fit with a single Lorentzian for the GaAs-like and GaP-like optical phonons (lines). As expected, the areas under the reststrahlen bands and the TO/LO splittings scale with composition. The Berreman artifact and some inteference effects are also seen.

Since a Lorentzian fit describes the data only qualitatively, we also fitted the ellipsometric angles with a Kramers-Kronig-consistent B-spline function²⁹ to approximate the dielectric function. The results are shown in Figs. S1 and 3. The TO peak heights and areas scale with composition, but the GaAs-like and GaP-like TO peaks are clearly separated for all compositions, as expected for two-mode behavior. The TO peaks are asymmetric and sometimes show weak sidebands. This could be in support of the cluster model¹⁰ or because of compositional variations in these HVPE-grown alloys.

The thickness, roughness parameters, high-frequency dielectric constant, TO and LO energies, and TO amplitudes and broadenings of GaAs-like and GaP-like phonon modes for ten different compositions are given in Table SI. Energies, amplitudes, and broadenings are shown in Fig. 4. For most samples, the LO energies agree very well with the Raman shifts from Pistol and Liu, ¹³ which confirms our use of the LST relation (2). The TO energies, which are not given in Ref. 13, were fitted with a linear relationship

$$\Omega_{\text{TO}}^{\text{GaP-like}} = 351.4(8) + 12.6(1.5)x \text{ meV},$$
 (3)

$$\Omega_{\text{TO}}^{\text{GaAs-like}} = 269.5 \pm 1.3 \text{ meV}. \tag{4}$$

The GaAs-like TO mode did not vary with composition within the errors of our data. The amplitudes of the TO modes scale approximately linearly with composition, as shown by the solid lines in Fig. 4 (b). The broadenings of the GaAs-like TO mode are small (about 5 cm⁻¹) across the entire range of compositions.

On the other hand, the broadenings of the GaP-like mode are large for small P contents and then decrease linearly with increasing x. This was also found by Verleur and Barker¹⁰ and is strong evidence in support of the cluster model. 14

We also determined the dielectric function and the complex refractive index of our $\mathrm{GaAs}_{1-x}\mathrm{P}_x$ alloy layers in the vicinity of the direct band gap E_0 and the dependence of E_0 on composition, $^{33-35}$ see Supplementary Material.

In summary, the infrared ellipsometry spectra of thick $GaAs_{1-x}P_x$ alloy layers grown on GaAs (001) by HVPE show strong GaAs-like and GaP-like reststrahlen bands due to optical phonon lattice absorption. The amplitudes and TO/LO phonon splittings vary with composition as expected. A model for the infrared dielectric function based on a single Lorentzian for each mode describes the ellipsometry data only qualitatively due to weak side bands, which are particularly pronounced for the GaP-like mode for low P contents. This is strong evidence in support of the Verleur and Barker cluster model. ^{10,14} There is insufficient information in our spectra to deconvolute our peaks into six to ten Lorentzians. A single additional GaP-like mode shifted by 12 meV, as suggested by the percolation model, ¹⁵ does not describe our data. Results for the optical constants near the direct band gap are also presented.

SUPPLEMENTARY MATERIAL

See the supplementary material for additional details about samples and methods, a detailed interpretation of the raw data for one sample, and visible ellipsometry results near the direct band gap.

ACKNOWLEDGMENTS

This research was supported in part by the Air Force Research Laboratory Sensors Directorate, through the Air Force Office of Scientific Research Summer Faculty Fellowship Program, Contract Numbers FA8750-15-3-6003, FA9550-15-0001 and FA9550-20-F-0005. VLT and SRV acknowledge support from the Air Force Office of Scientific Research (Program Manager Dr. John Luginsland) under award number FA9550-22RYCOR003. We are grateful to Dr. T. E. Tiwald for guiding us through the use of B-spline functions for fitting IR ellipsometry data.

¹A. H. Kachare, W. G. Spitzer, F. K. Euler, and A. Kahan, J. Appl. Phys. 45, 2938 (1974).

²R. T. Holm, J. W. Gibson, and E. D. Palik, J. Appl. Phys. 48, 212 (1977).

³E. D. Palik, in Handbook of Optical Constants of Solids, edited by E. D. Palik (Academic, New York, 1998), p. 429.

⁴D. J. Lockwood, G. Yu, and N. L. Rowell, Solid State Commun.

⁵A. S. Barker, Phys. Rev. **165**, 917 (1968).

⁶N. S. Samarasingha and S. Zollner, J. Vac. Sci. Technol. B 39, 052201 (2021)

⁷L. Genzel, T. P. Martin, and C. H. Perry, phys. stat. sol. (b) **62**, 83 (1974).

⁸I. F. Chang and S. S. Mitra, Adv. Phys. 20, 359 (1971).

⁹J. Humlíček, Thin Solid Films **313–314**, 687 (1998).

Applied Physics Letters

This is the author's peer reviewed, accepted manuscript. However, the online version of record will be different from this version once it has been copyedited and typeset PLEASE CITE THIS ARTICLE AS DOI: 10.1063/5.0173978

- ¹⁰H. W. Verleur and A. S. Barker, Phys. Rev. **149**, 715 (1966). ¹¹Y. S. Chen, W. Schockley, and G. L. Pearson, Phys. Rev. 151,648 ¹²N. D. Strahm and A. L. McWorter, in *Proceedings of the Con*ference on Light Scattering Spectra In Solids, edited by G. B. Wright (Springer, New York, 1969), p. 455.
- M. E. Pistol and X. Liu, Phys. Rev. B 45, 4312 (1992).
 J. Cebulski, M. Woźny, and E. M. Sheregii, phys. stat. sol. (b)
- 250, 1014 (2015).
 150, Pagès, J. Souhabi, A. V. Postnikov, and A. Chafi, Phys. Rev. B 80, 035204 (2009).
- ¹⁶R. Schmidt-Grund, M. Schubert, B. Rheinländer, D. Fritsch, H. Schmidt, E. M. Kaidashev, M. Lorenz, C. M. Herzinger, and M. Grundmann, Thin Solid Films 455-456, 500 (2004).
- ¹⁷S. Schöche, T. Hofmann, D. Nilsson, A. Kakanakova-Georgieva, E. Janzén, P. Kühne, K. Lorenz, M. Schubert, and V. Darakchieva, J. Appl. Phys. 121, 205701 (2017).
 ¹⁸M. Stokey, T. Gramer, R. Korlack, S. Knight, S. Richter, R.
- Jinno, Y. Cho, H. G. Xing, D. Jena, M. Hilfiker, V. Darakchieva, and M. Schubert, Appl. Phys. Lett. **120**, 112202 (2022).

 ¹⁹M. G. Craford, R. W. Shaw, A. H. Herzog, and W. O. Groves,
- J. Appl. Phys. 43, 4075 (1972).
- Appl. Phys. 49, 4010 (1912).
 V. Petrov, Prog. Quantum Electron. 42, 1 (2015).
 L. Wang, S. R. Vangala, S. Popien, M. Beutler, V. L. Tassev, and V. Petrov, phys. stat. sol. RRL 16, 2200198 (2022).

- ²²A. Strömberg, G. Omanakuttan, Y. Liu, T. Mu, Z. Xu, S. Lourdudoss, and Y.-T. Sun, J. Cryst. Growth 540, 125623 (2020).
- ²³V. L. Tassev and S. R. Vangala, Crystals **9**, 393 (2019)
- I. I assev and S. R. Vangana, Cystan V, 500 (2015).
 Tassev, S. Vangala, D. Brinegar, M. Parker, and T. Barlow, phys. stat. sol. (a) 218, 2000443 (2021).
 V. Petrov, L. Wang, S. Vangala, and V. Tassev, Proc. SPIE
- **11985**, 1198506 (2022).
- ²⁶I. Vurgaftman, J. R. Meyer, and L. R. Ram-Mohan, J. Appl. Phys. 89, 5815 (2001).
- Flys. 69, 361 (2001).
 27A. G. Thompson, M. Cardona, K. L. Shaklee, and J. C. Woolley,
 Phys. Rev. 146, 601 (1966).
- ²⁸D. E. Aspnes, Phys. Rev. B **14**, 5331 (1976).
- F. Hispaco, A. M. Collins, Spectroscopic Ellipsometry for Photovoltaics Vol. 1 (Springer, Cham, 2018).
 T. I. Willett-Gies, C. M. Nelson, L. S. Abdallah, and S. Zollner,
- J. Vac. Sci. Technol. A 33, 061202 (2015).
- ³¹D. W. Berreman, Phys. Rev. **130**, 2193 (1963)
- ³²J. Humlíček, phys. stat. sol. (b) **215**, 155 (1999).
- ³³S. Zollner, J. Kircher, M. Cardona, and S. Gopalan, Solid-State Electron, 32, 1585 (1989).
- ³⁴S. Zollner, M. Garriga, J. Kircher, J. Humlíček, M. Cardona, and G. Neuhold, Phys. Rev. B 48, 7915 (1993).
- Neumond, Lays. Rev. D 39, 100 (1995)
 S. Zollner, P.P. Paradis, F. Abadizaman, and N.S. Samarasingha,
 J. Vac. Sci. Technol. B 37, 012904 (2019).